

Quantum theory of reactive scattering and adsorption at surfaces

Axel Groß

Physik-Department T30, TU München, 85747 Garching, Germany

The interaction of atoms and molecules with surfaces is of great technological relevance. For a reliable theoretical description of the interaction dynamics of light atoms and molecules such as hydrogen or helium with surfaces, quantum effects have to be taken into account. In this article, I will discuss quantum effects in the interaction dynamics of both the substrate as well as the incident particles. There are pure quantum phenomena such as elastic scattering and diffraction. Elastic scattering, i.e. scattering without any energy transfer to the substrate, is a consequence of the quantum nature of the substrate vibrations, the phonons. It is particularly important in the trapping of noble gas atoms at surfaces. In the case of elastic scattering at a periodic surface, the momentum parallel to the surface is conserved within multiples of the reciprocal lattice vectors. This leads to diffraction, i.e. to a characteristic pattern of well-resolved scattering peaks. Further quantum effects that influence the scattering and reaction probabilities are threshold effects due to the opening up of new scattering channels, scattering resonances, tunneling, zero-point vibrations and quantization effects at transition states. These quantum effects will be discussed using the adsorption of rare gas atoms and the scattering and dissociative adsorption of hydrogen as examples.

I. INTRODUCTION

The interaction of atoms and molecules with surfaces is of great technological relevance [1]. Both advantageous and harmful processes can occur at surfaces. Catalytic reactions at surfaces represent a desired process while corrosion is an unwanted process. If light atoms and molecules such as hydrogen or helium are interacting with the surface, then quantum effects in the interaction dynamics between the incoming beam and the substrate have to be taken into account. First of all there are quantum effects in the energy transfer to the substrate vibrations, the phonons. While classically there will always be an energy loss of the incident particles to the substrate, quantum mechanically there is a certain probability for elastic scattering, i.e. without any energy transfer between the substrate and the scattered particles. This has also important consequences on the sticking probabilities of weakly bound species such as rare gases at low kinetic energies.

Furthermore, in elastic scattering at a periodic surface, the wave vector parallel to the surface can only be changed by reciprocal lattice vectors because of the quasi-momentum conservation. If the de Broglie wavelength of the incident particles is of the order of the lattice spacing of the substrate, the angular distribution of the scattered particles exhibits a characteristic pattern of well-resolved reflection peaks. The resulting diffraction pattern depends only on the geometry of the surface. Therefore it has been used extensively as a tool to determine surface structures [2, 3].

I will first address quantum effects in the sticking of weakly bound species, namely rare gas atoms, at surfaces. Depending on the mass of the rare gas atoms, the whole range between almost purely classical and almost purely quantum behavior can be observed [4, 5]. The lighter the atom, the higher the probability for elastic scattering and therefore the lower the trapping probability. I will also briefly mention quantum effects in the

adsorption dynamics which in fact lead to a vanishing trapping probability in the limit of very low incident kinetic energies and surface temperatures [6–9]

As far as quantum effects in the dynamics of the scattered particles are concerned, I will use the interaction of hydrogen with palladium surfaces as a model system. This system has been well-studied both experimentally and theoretically. Initially these studies were motivated among other reasons by the fact that bulk palladium can absorb huge amounts of hydrogen. This made it a possible candidate for a hydrogen storage device in the context of the fuel cell technology. Besides, palladium is also used as a catalyst material for hydrogenation and dehydrogenation reactions.

The strong corrugation and anisotropy of the $\text{H}_2/\text{Pd}(100)$ potential energy surface (PES) lead to significant off-specular and rotationally inelastic diffraction intensities [10]. These effects have been verified for related reactive systems [11, 12]. Furthermore, the diffraction intensities exhibit a pronounced oscillatory structure because of threshold effects and resonances in the scattering process. This structure is also visible in the quantum mechanically determined adsorption probability of $\text{H}_2/\text{Pd}(100)$ [10, 13, 14]. This, however, has not been found in experiments yet [15]. Further quantum effects in activated systems are due to the localization and quantization of the wave function in the barrier region [16, 17] which causes a steplike structure in the reaction probabilities.

This paper is structured as follows. In the next section, a general introduction into the phenomena occurring in the quantum scattering at surfaces will be given. Then quantum effects in the trapping at surfaces will be addressed. After the section about diffraction, the influence of quantum phenomena in the reaction dynamics at surfaces will be discussed. The paper ends with some concluding remarks.

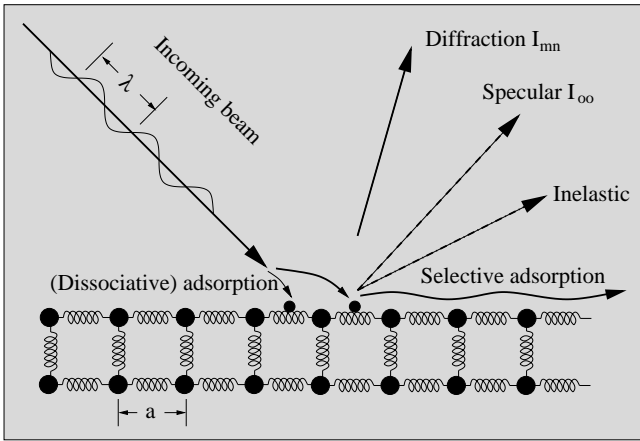


FIG. 1: Summary of the different collision processes in reactive scattering at surfaces.

II. QUANTUM SCATTERING AT SURFACES

A schematic summary of possible collision processes in the scattering of atoms and molecules at surfaces is presented in Fig. 1. We consider a monoenergetic beam of atoms or molecules impinging on a periodic surface. In the following, we will refer to both atoms and molecules by just calling them molecules. A monoenergetic incident beam is characterized by the wave vector $\vec{K}_i = \vec{P}_i/\hbar$, where \vec{P}_i is the initial momentum of the particles. When the incoming particles hit the surface, the substrate atoms will recoil. Therefore, classically there will always be a certain energy transfer from the molecules to the substrate. Quantum mechanically, however, there will be a certain probability for elastic scattering, i.e. with no energy transfer to the substrate. This probability is given by the so-called Debye-Waller factor.

Furthermore, if the de Broglie wavelength $\lambda = 1/|\vec{K}_i|$ of the incident beam is of the order of the lattice spacing a , quantum effects in the momentum transfer parallel to the surface become important. In the case of elastic scattering, the component of the wave vector parallel to the surface can only be changed by a reciprocal lattice vector of the periodic surface. This means that the wave vector \vec{K}_f^{\parallel} after the scattering is given by

$$\vec{K}_f^{\parallel} = \vec{K}_i^{\parallel} + \vec{G}_{mn}, \quad (1)$$

where \vec{G}_{mn} is a reciprocal lattice vector of the periodic surface. The conservation of the quasi-momentum parallel to the surface in elastic scattering leads to diffraction which means that there is only a discrete number of allowed scattering angles. The intensity of the elastic diffraction peak mn according to (1) is denoted by I_{mn} . The scattering peak I_{00} with $\vec{K}_f^{\parallel} = \vec{K}_i^{\parallel}$ is called the *specular peak*.

From the diffraction pattern the periodicity and lattice constant of the surface can be derived. The coherent

scattering of atoms or molecules from surfaces has been known as a tool for probing surface structures since 1930 [18]. In particular helium atom scattering (HAS) has been used intensively to study surface crystallography (see, e.g., [2] and references therein).

The main source for the energy transfer between the impinging molecules and the substrate is the excitation and deexcitation of substrate phonons. Phonons also carry momentum. Then the conservation of quasi-momentum parallel to the surface reads

$$\vec{K}_f^{\parallel} = \vec{K}_i^{\parallel} + \vec{G}_{mn} + \sum_{\text{exch. phon.}} \pm \vec{Q}, \quad (2)$$

where \vec{Q} is a two-dimensional phonon-momentum vector parallel to the surface. The plus-signs in the sum correspond to the excitation or emission of a phonon while the minus-signs represent the deexcitation or absorption of a phonon. The energy balance in phonon-inelastic scattering can be expressed as

$$\frac{\hbar^2 \vec{K}_f^2}{2M} = \frac{\hbar^2 \vec{K}_i^2}{2M} + \sum_{\text{exch. phon.}} \pm \hbar\omega_{\vec{Q},j}, \quad (3)$$

where $\hbar\omega_{\vec{Q},j}$ corresponds to the energy of the phonon with momentum \vec{Q} and mode index j . In fact, helium atom scattering has been used extensively in order to determine the surface phonon spectrum in one-phonon collisions via Eqs. (2) and (3) [2, 19].

The excitation of phonons usually leads to a reduced normal component of the kinetic energy of the back-scattered atoms or molecules. Thus the reflected beam is shifted in general to larger angles with respect to the surface normal compared to the angle of incidence. The resulting supraspecular scattering is indicated in Fig. 1 as the inelastic reflection event.

In the case of the scattering of weakly interacting particles at smooth surfaces, often resonances in the intensity of the specular peak as a function of the angle of incidence are observed [20]. These so-called *selective adsorption resonances* which are also indicated in Fig. 1 occur when the scattered particle can make a transition into one of the discrete bound state of the adsorption potential [21]. This is only possible if temporarily the motion of the particle is entirely parallel to the surface. The interference of different possible paths along the surface causes the resonance effects. Energy and momentum conservation yields the selective adsorption condition

$$\frac{\hbar^2 \vec{K}_i^2}{2M} = \frac{\hbar^2 (\vec{K}_i^{\parallel} + \vec{G}_{mn})^2}{2M} - |E_l|, \quad (4)$$

where E_l is a bound level of the adsorption potential. From the scattering resonances, bound state energies can be obtained using Eq. 4 without any detailed knowledge about the scattering process.

The coherent elastic scattering of molecules is more complex than atom scattering. Additional peaks may

appear in the diffraction pattern. These are a consequence of the fact that in addition to parallel momentum transfer the internal degrees of freedom of the molecule, rotations and vibrations, can be excited during the collision process. The total energy balance in the molecular scattering is

$$\frac{\hbar^2 \vec{K}_f^2}{2M} = \frac{\hbar^2 \vec{K}_i^2}{2M} + \Delta E_{\text{rot}} + \Delta E_{\text{vib}} + \sum_{\text{exch.phon.}} \pm \hbar \omega_{\vec{Q},j}. \quad (5)$$

Usually the excitation of molecular vibrations in molecule-surface scattering is negligible, in contrast to the phonon excitation. This is due to the fact that the time-scale of the molecular vibrations is usually much shorter than the scattering time or the rotational period. This leads to high frequencies of the molecular vibrations whose energies are too high to become excited in a typical scattering experiment. Molecular rotations, on the other hand, can be excited rather efficiently in the scattering at highly corrugated and anisotropic surfaces. Because of the energy conservation, the rotational excitation in scattering reduces the kinetic energy perpendicular to the surface. This leads to additional peaks in the diffraction spectrum, the *rotationally inelastic diffraction* peaks.

Experimentally, rotationally inelastic diffraction of hydrogen molecules has been first observed in the scattering at inert ionic solids such as MgO [22] or NaF [23]. At metal surfaces with a high barrier for dissociative adsorption, the molecules are scattered at the tails of the metal electron density which are usually rather smooth. In addition, the interaction of the molecules with these tails does not depend very strongly on the orientation of the molecules. Hence relatively weak diffraction and hardly any rotationally inelastic diffraction has been observed for, e.g., the scattering of H₂ from Cu(001) [24, 25]. This is different for the case of HD scattering, where the displacement of the center of mass from the center of the charge distribution leads to a strong rotational anisotropy [26].

At reactive surfaces where non-activated adsorption is possible, the scattering occurs rather close to the surface where the potential energy surface is already strongly corrugated and anisotropic. For such systems, rotationally inelastic peaks in the diffraction pattern have been clearly resolved experimentally [11, 12] and predicted theoretically in six-dimensional quantum dynamical calculations [10] as will be discussed below.

At reactive surfaces, the particles can off course also adsorb. As it is indicated in Fig. 1, molecules can adsorb both molecularly which means intact or dissociatively. In the case of the atomic or molecular adsorption, the particles can only remain trapped at the surface if their initial kinetic energy is transferred to the surface and dissipated. For light projectiles, the quantum nature of the substrate phonons becomes important. This will be the topic of the next section.

III. QUANTUM EFFECTS IN THE TRAPPING AT SURFACES

Let us consider an atom impinging on a surface. Even in the absence of any chemical binding, there will always be an attractive interaction between the surface and the atom due to the van der Waals forces [27]. Let us further assume that there is no energetic barrier for the access of the atomic adsorption well. A particle impinging on a surface can only become trapped in an attractive adsorption well if it transfers its entire initial kinetic energy to the surface because then it cannot escape back to the gas phase. Hence the sticking probability can be expressed as

$$S(E) = \int_E^\infty P_E(\epsilon) d\epsilon, \quad (6)$$

where $P_E(\epsilon)$ is the probability that an incoming particle with kinetic energy E transfers the energy ϵ to the surface.

If the adsorption process is treated purely classical, no matter how small the adsorption well, no matter how small the mass ratio between the impinging atom and the substrate oscillator, for $E \rightarrow 0$ and $T_s \rightarrow 0$ the sticking probability will always reach unity if there is no barrier before the adsorption well. This is due to the fact that every impinging particle will transfer energy to the substrate at zero temperature. In the limit of zero initial kinetic energy any energy transfer will be sufficient to keep the particle in the adsorption well. Quantum mechanically, however, there is a non-zero probability for elastic scattering at the surface. Hence the sticking probabilities should become less than unity in the zero-energy limit, in particular for light atoms impinging on a surface. This has indeed been observed in the sticking of rare gas atoms at cold Ru(0001) surfaces [4, 5].

In order to reproduce elastic scattering, the quantum nature of the phonon system has to be taken into account. In the simplest approach, the substrate phonons can be modeled by an ensemble of independent quantum surface oscillators. Since the oscillators are assumed to be independent, the essential physics can be captured by just considering an atomic projectile interacting via linear coupling with a single surface oscillator. In the so-called trajectory approximation, the particle's motion is treated classically. Assuming that the motion of the atom is hardly influenced by the excitation of the surface oscillator, the equation of motion are solved without taking the coupling to the oscillator into account. The classical trajectory then introduces a time-dependent force in the Hamiltonian of the oscillator. In this *forced oscillator model* [28], the energy transfer probability $P_E(\epsilon)$ can be evaluated.

In fact, a compact expression can be derived for the energy distribution in the scattering of an atom at a system of phonon oscillators with a Debye spectrum at a temperature T_s [29, 30]. Assuming some analytical form for the potential, this expression depends on a small set

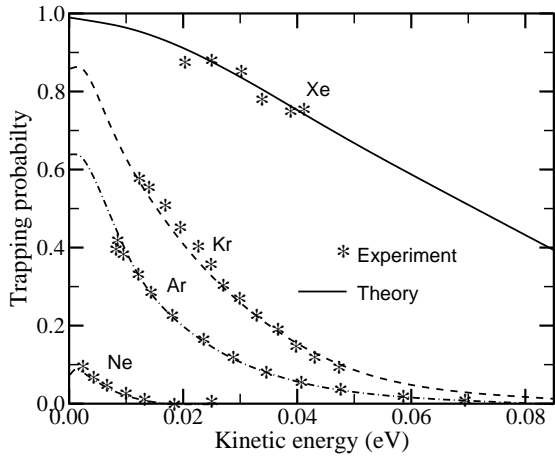


FIG. 2: Sticking probability of rare gas atoms on Ru(0001) at a surface temperature of $T_s = 6.5$ K. Stars (*): experiment; lines: theoretical results obtained with the forced oscillator model (after [5], not all measured data points are included)

of parameters such as the potential well depth, the potential range, the mass of the surface oscillator and the surface Debye temperature. This model was used in order to reproduce the measured sticking probabilities of rare gas atoms on a Ru(001) surface at a temperature of $T_s = 6.5$ K [5].

A comparison between the measured and calculated sticking probabilities for Ne, Ar, Kr and Xe on Ru(001) is shown in Fig. 2. The lighter the atoms, the smaller the sticking probability. At small energies, the sticking probabilities do not reach unity due to the quantum nature of the substrate phonons except for the heaviest rare gas atom Xe. Indeed, attempts to reproduce the measured sticking probabilities with purely classical methods have failed, at least for Ne and Ar [4, 5]. A classical treatment of the solid is only appropriate if the energy transfer to the surface is large compared to the Debye energy of the solid [6].

At even lower kinetic energies than reached in the experiments [5] shown in Fig. 2, the quantum nature of the impinging particles cannot be neglected any longer. Hence the trajectory approximation cannot be applied any more. In fact, in the limit $E \rightarrow 0$ the de Broglie wavelength of the incoming particle tends to infinity. In the case of a short-range attractive potential this means that the amplitude of the particle's wave function vanishes in the attractive region [6, 7]. Thus there is no coupling and consequently no energy transfer between the particle and the substrate vibrations. Therefore the quantum mechanical sticking probability also vanishes for $E \rightarrow 0$. However, in order to see this effect extremely small kinetic energies corresponding to a temperature below 0.1 K are required [6]. Nevertheless, this quantum phenomenon in the sticking at surfaces has been verified experimentally for the adsorption of atomic hydrogen on thick liquid ^4He films [31].

There is yet another effect that also leads to zero stick-

ing at very low energies. Quantum mechanically particles can also be reflected at attractive parts of the potential. If the potential falls off asymptotically faster than $1/Z^2$, then the reflection amplitude R exhibits the universal behavior [9, 32]

$$|R| \xrightarrow[k \rightarrow 0]{} 1 - bk, \quad (7)$$

where k is the wave number corresponding to the asymptotic kinetic energy $E = \hbar^2 k^2 / 2M$. This means that in the low energy limit the reflection probability $|R|^2$ goes to unity even if the particle does not reach a classical turning point. In fact, such a *quantum reflection* has been observed in the scattering of an ultracold beam of metastable neon atoms from silicon and glass surfaces [8]. In order to reproduce the measured reflectivities, an $1/Z^4$ dependence of the potential has to be assumed [8, 9] where Z is the distance to the surface. This indicates that the atoms are scattered at the long-range tail of the so-called Casimir-van der Waals potential.

IV. DIFFRACTION

In order to describe diffraction, the wave nature of the scattered molecules have to be taken into account by solving the appropriate Schrödinger equation. Either the time-dependent Schrödinger equation

$$i\hbar \frac{\partial}{\partial t} \Psi(\vec{R}, t) = H \Psi(\vec{R}, t) \quad (8)$$

or the time-independent Schrödinger equation

$$H \Psi(\vec{R}) = E \Psi(\vec{R}, t) \quad (9)$$

may be considered to treat the scattering process. The time-dependent Schrödinger equation is typically solved on a numerical grid using the wave-packet formalism [33–36]. In the time-independent formulation, the wavefunction is usually expanded in some suitable set of eigenfunctions leading to so-called *coupled-channel equations* [27, 37].

One important prerequisite for the determination of scattering intensities is the knowledge of the interaction potential between the scattered particles and the surface. While about one decade ago most interaction potentials had to be guessed based on experimental information, it has now become possible to map out whole potential energy surfaces by *ab initio* total-energy calculations [37, 38] which is illustrate in Fig. 3. This development has been caused by the progress in computer power and by the development of efficient electronic structure codes (see, e.g., Refs. [39–42]).

I will use the scattering of H_2 at a metal surface as an exemplary system to discuss the quantum effects in the scattering at surfaces. While a decade ago it was still not possible to perform full quantum dynamical simulations in all hydrogen degrees of freedom, this can

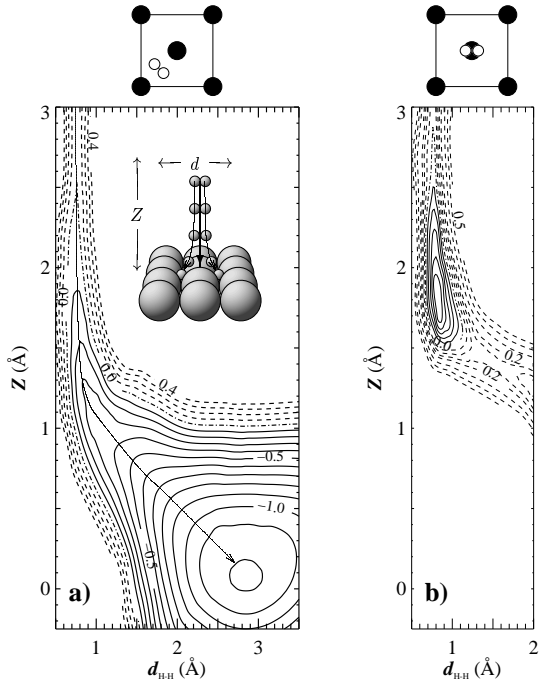


FIG. 3: Contour plots of the PES along two two-dimensional cuts through the six-dimensional coordinate space of $\text{H}_2/\text{Pd}(100)$ (from [49]). The contour spacing is 0.1 eV per H_2 molecule. The considered coordinates are indicated in the inset. The lateral position of the H_2 molecule and its orientation are indicated above the contour plots.

now be routinely done [13, 43–47]. In particular, hydrogen/palladium represents a system that is well-suited for both experiments under ultra-high vacuum conditions as well as for a theoretical treatment in the framework of modern electronic structure methods. There is a wealth of microscopic information which is well established and double-checked through the fruitful combination of state-of-the-art experiments with *ab initio* total-energy calculations and related simulations. The interaction potential of hydrogen interacting with palladium surfaces has been determined in detail by several total-energy calculations [48–51] based on density-functional theory. Parametrizations of the *ab initio* potential energy surfaces have been used for quantum and classical molecular dynamics simulations of the scattering and adsorption of H_2 on $\text{Pd}(100)$ [10, 13, 14], $\text{Pd}(111)$ [52–54] and $\text{Pd}(110)$ [55].

In this contribution, I will particularly focus on $\text{H}_2/\text{Pd}(100)$. Two so-called elbow potentials of this system which were determined by DFT calculations [49, 56] are shown in Fig. 3. The $\text{H}_2/\text{Pd}(100)$ PES which is a six-dimensional hyperplane according to the H_2 degrees of freedom when the substrate atoms are kept fixed is usually analysed in terms of these elbow potentials. They correspond to two-dimensional cuts through the six-dimensional PES as a function of the molecular distance from the surface Z and the interatomic H-H dis-

tance r for fixed lateral center-of-mass coordinates and molecular orientation.

Hydrogen molecules usually adsorb dissociatively on metal surfaces [57, 58]. As Fig. 3a indicates, H_2 dissociates spontaneously at $\text{Pd}(100)$, i.e. there are non-activated paths for dissociative adsorption. However, dissociative adsorption corresponds to a bond making-bond breaking process that depends sensitively on the local chemical environment. Consequently, the PES is strongly corrugated which means the interaction strongly varies as a function of the lateral coordinates of the molecule. This illustrated in Fig. 3b. If the molecules comes down over the on-top site, the shape of the elbow looks entirely different. Along this pathway, the adsorption is no longer non-activated. We will see that the strong corrugation leads to significant intensities in the off-specular peaks.

The PES does not only depend on the lateral position of the H_2 molecule, i.e., the PES is not only corrugated, but it is also strongly anisotropic. Only molecules with their axis parallel to the surface can dissociate, for molecules approaching the Pd surface in an upright orientation the PES is purely repulsive [49]. Because of the anisotropy of the PES, in addition to elastic diffraction peaks there will be large intensities in rotationally inelastic diffraction peaks which correspond to rotational transitions in the collision process.

The six-dimensional *ab initio* PES of $\text{H}_2/\text{Pd}(100)$ has been parametrized using some suitable analytical form [14]. Using this fit, the six-dimensional quantum dynamics of H_2 interacting with a fixed substrate have been determined [10] by solving the time-independent Schrödinger equation in a coupled-channel scheme using the concept of the so-called *local reflection matrix* (LORE) [59, 60]. This is a numerically very efficient and stable scheme that is based on a fine step-wise representation of the PES.

One typical calculated angular distribution of H_2 molecules scattered at $\text{Pd}(100)$ is shown in Fig. 4 [10]. The total initial kinetic energy is $E_i = 76$ meV. The incident parallel momentum equals $2\hbar G$ along the $\langle 0\bar{1}1 \rangle$ direction which corresponds to an incident angle of $\theta_i = 32^\circ$. The molecules are initially in the rotational ground state $j_i = 0$. Figure 4a shows the so-called in-plane scattering distribution, i.e. the diffraction peaks in the plane spanned by the wave vector of the incident beam and the surface normal. The label (m, n) denotes the parallel momentum transfer $\Delta\mathbf{G}_{\parallel} = (mG, nG)$. The specular peak is the most pronounced one, but the first order diffraction peak (10) is only a factor of four smaller. Note that in a typical helium atom scattering experiment the off-specular peaks are about two orders smaller than the specular peak [2]. This is due to the fact that the chemically inert helium atoms are scattered at the smooth tails of the surface electron distribution.

In addition, rotationally inelastic diffraction peaks corresponding to the rotational excitation $j = 0 \rightarrow 2$ are plotted in Fig. 4a. They have been summed up over all final azimuthal quantum numbers m_j . Note that the exci-

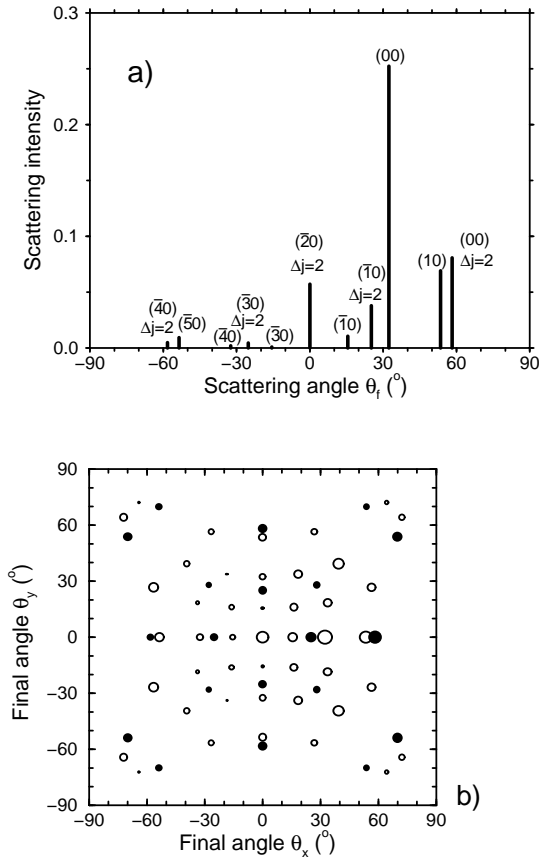


FIG. 4: Six-dimensional quantum results of the rotationally inelastic scattering of H_2 on Pd(100) for a kinetic energy of 76 meV at an incidence angle of 32° along the [10] direction of the square surface lattice. Panel a) shows the in-plane diffraction spectrum where all peaks have been labeled according to the transition. Both in-plane and out-of-plane diffraction peaks are plotted in panel b) the open and filled circles correspond to the rotationally elastic and rotationally inelastic scattering, respectively. The radius of the circles is proportional to the logarithm of the scattering intensity (after [10]).

tation probability of the so-called cartwheel rotation with $m = 0$ is for all peaks approximately one order of magnitude larger than for the so-called helicopter rotation $m = j$, since the polar anisotropy of the PES is stronger than the azimuthal one. The intensity of the rotationally inelastic diffraction peaks in Fig. 4 is comparable to the rotationally elastic ones. Except for the specular peak they are even larger than the corresponding rotationally elastic diffraction peak with the same momentum transfer (m, n) . Because of the particular conditions with the incident parallel momentum corresponding to the reciprocal lattice vector $\vec{G}_{\parallel} = (2G, 0)$, the rotationally elastic and inelastic $(\bar{2}0)$ diffraction peaks fall upon each other.

The out-of-plane scattering intensities are not negligible, which is demonstrated in Fig. 4b. The open circles represent the rotationally elastic, the filled circles the ro-

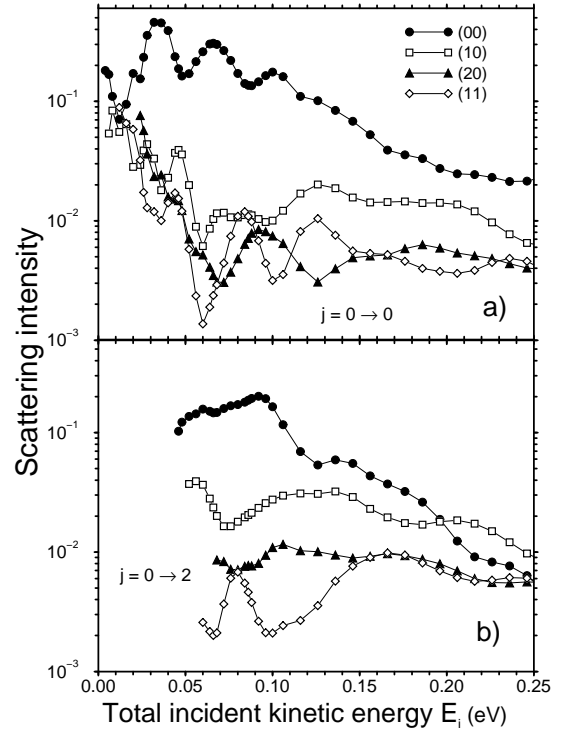


FIG. 5: Calculated scattering intensity versus kinetic energy for H_2 molecules in the rotational ground state impinging under normal incidence on Pd(100) with an initial velocity spread of $\Delta v/v = 0.05$ (after [10]).

tationally inelastic diffraction peaks. The radii of the circles are proportional to the logarithm of the scattering intensity. The sum of all out-of-plane scattering intensities is approximately equal to the sum of all in-plane scattering intensities. Interestingly, some diffraction peaks with a large parallel momentum transfer still show substantial intensities. This phenomenon is well known from helium atom scattering and has been discussed within the concept of so-called rainbow scattering [61].

The intensity of the scattering peaks for normal incidence are analysed in detail in Fig. 5. The intensities of four diffraction peaks are plotted as a function of the kinetic energy for rotationally elastic (Fig. 5a) and rotationally inelastic (Fig. 5b) scattering. In molecular beam experiments, the beams are not monoenergetic but have a certain velocity spread. In order to allow a better comparison with the experiment, an initial velocity spread of $\Delta v/v = 0.05$ typical for experiments [12] has been applied to the results of the quantum dynamical simulations.

The theoretical results still exhibit a rather strong oscillatory structure which is a consequence of the quantum nature of H_2 scattering. Let us first focus on the specular peak. An analysis of the energetic position of the oscillations reveals that they occur whenever new diffraction channels open up. This process is illustrated in Fig. 6.

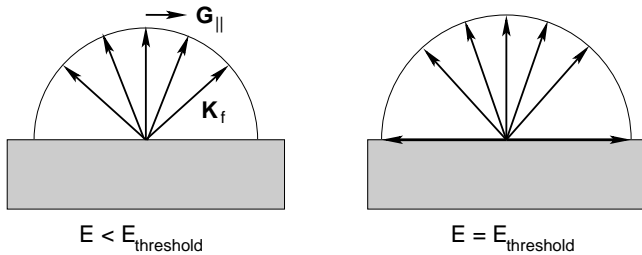


FIG. 6: Schematic illustration of the opening up of new scattering channels for normal incidence as a function of the energy.

For a particular kinetic energy, there is a discrete number of diffraction peaks. The final wave vectors \vec{K}_f differ by multiples of the unit vectors \vec{G}_{\parallel} of the reciprocal lattice. At certain threshold energies $E_{\text{threshold}}$ the energy becomes large enough that additional diffraction channels open up. At exactly $E = E_{\text{threshold}}$, the new channel corresponds to a wave that propagates parallel to the surface. Thus the oscillations in the scattering intensities are a consequence of the fact that at the threshold energies the number of diffraction peaks changes discontinuously.

In detail, the first pronounced dip in the intensity of the specular peak at $E_i = 12$ meV coincides with the emergence of the (11) diffraction peak, the small dip at $E_i = 22$ meV with the opening up of the (20) diffraction channel. The huge dip at approximately $E_i = 50$ meV reflects the threshold for rotationally inelastic scattering. Interestingly, the rotational elastic (10) and (11) diffraction peaks show pronounced maxima at this energy. This indicates a strong coupling between parallel motion and rotational excitation.

Figure 5b shows the intensities of the rotationally inelastic diffraction peaks. The specular peak is still the largest, however, some off-specular peaks become larger than the (00) peak at higher energies. This is due to the fact that the rotationally anisotropic component of the potential is more corrugated than the isotropic component [49]. Besides, it is apparent that the oscillatory structure for rotationally inelastic scattering is somewhat smaller than for rotationally elastic scattering.

Not all peaks in the scattering amplitudes can be unambiguously attributed to the emergence of new scattering channels. As already mentioned in section II, additional structures in the scattering intensities can also be caused by selective adsorption resonances: molecules become temporarily trapped into metastable molecular adsorption states at the surface due to the transfer of normal momentum to parallel and angular momentum which resonantly enhances the scattering intensities. Such resonances have been clearly resolved, e.g. in the physisorption of H_2 on Cu [62]. For the strongly corrugated and anisotropic $\text{H}_2/\text{Pd}(100)$ system it is difficult to identify the nature of possible scattering resonances from the quantum calculations. Classically, one observes dynamic

trapping in the H_2/Pd interaction dynamics [52, 53, 63] which is the equivalent of selective adsorption resonances: impinging molecules do neither directly scatter nor dissociate but transfer energy from the translation perpendicular to the surface into internal degrees of freedom and motion parallel to the surface. In this transient state, they can spend several ps at the surface. Although most of the dynamically trapped molecules eventually dissociate, this process still influences the reflection probabilities.

Oscillatory structures have been known for years in He and H_2 scattering [20] and also in low-energy electron diffraction (LEED) [64]. For reactive systems such as $\text{H}_2/\text{Pd}(100)$, the experimental observation of diffraction is not trivial. Because of the reactivity, an adsorbate layer builds up very rapidly during the experiment. These layers destroy the perfect periodicity of the surface and thus suppress diffraction effects. In order to keep the surface relatively clean, one has to use rather high surface temperatures so that adsorbates quickly desorb again. High surface temperatures, on the other hand, also smear out the diffraction pattern. Still experimentalists managed to clearly resolve rotationally inelastic peaks in the diffraction pattern of $\text{D}_2/\text{Ni}(110)$ [12] and $\text{D}_2/\text{Rh}(110)$ [11] in addition to rotationally elastic peaks.

V. QUANTUM EFFECTS IN REACTION PROBABILITIES

While elastic scattering and diffraction are purely quantum phenomena that cannot be understood and reproduced within classical physics, reaction probabilities can be calculated by both classical and quantum molecular dynamics calculations. In a multidimensional situation, classical reaction probabilities are obtained by averaging over molecular dynamics simulations for statistically distributed initial conditions. For example, to determine the probability for dissociative adsorption, trajectories with different initial lateral position within the surface unit cell and different molecular orientations have to be run. A quantum wave function, on the other hand, is always delocalized to a certain degree. One could say that quantum reaction probabilities correspond to coherent average over initial conditions while classically the average is done incoherently. This coherent averaging causes quantum effects for example in the dissociative adsorption probability that will be discussed in this section.

We will continue to focus on the system $\text{H}_2/\text{Pd}(100)$. In the determination of the diffraction pattern, we had neglected the substrate motion. This approximation is indeed justified in the description of the interaction of hydrogen with densely packed metal surfaces. There is only a small energy transfer from the light hydrogen molecule to the heavy substrate atoms. Furthermore, usually no significant surface rearrangement occurs during the interaction time. Even in the description of the dissociative adsorption of H_2 on metal surfaces, in contrast to

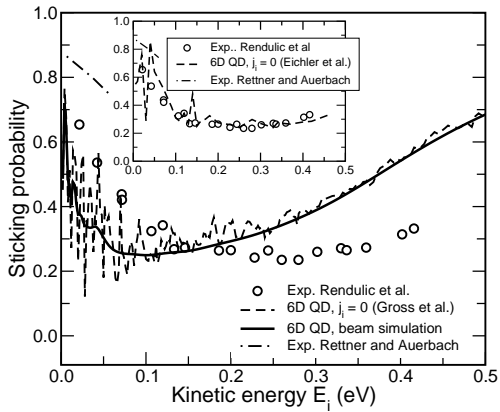


FIG. 7: Sticking probability of $\text{H}_2/\text{Pd}(100)$ as a function of the initial kinetic energy. Circles: H_2 molecular beam adsorption experiment under normal incidence (Rendulic *et al.* [65]); dash-dotted line: H_2 effusive beam scattering experiment with an incident angle of $\theta_i = 15^\circ$ (Rettner and Auerbach [15]) dashed and solid line: theory according to H_2 initially in the ground state and with a thermal distribution appropriate for a molecular beam [13]. The inset shows the theoretical results using an improved *ab initio* potential energy surface [45].

molecular adsorption, the substrate motion can be safely neglected [36, 37, 58]. The crucial process in the dissociative adsorption dynamics is the bond-breaking process, i.e. the conversion of translational and internal energy of the hydrogen molecule into translational energy of the atomic fragments on the surface relative to each other. The fragments will of course eventually thermalize at the surface by transferring their excess energy to the substrate, but this only occurs after the dissociation step. Thus the dissociation dynamics can be described by a six-dimensional PES which takes only the molecular degrees of freedom into account.

In this framework, the dissociation probability can be regarded as a quantum transmission probability from the entrance channel of the impinging molecule to the dissociation channel at the surface. Because of the conservation of the particle flux, the adsorption probability for some particular initial state i can be evaluated by

$$S_i = 1 - \sum_j |R_{ji}|^2, \quad (10)$$

where the R_{ji} are the amplitudes of all final scattering states. The calculated dissociative adsorption probability of $\text{H}_2/\text{Pd}(100)$ as a function of the kinetic energy is shown in Fig. 7 and compared to the results of molecular beam experiments [15, 65]. The inset shows more recent results using an improved *ab initio* potential energy surface [45].

Because of the unitarity relation Eq. (10), scattering and adsorption probabilities are closely linked to each other. Indeed, the adsorption probability also exhibits a pronounced oscillatory structure at exactly the same kinetic energies as the scattering intensities. This means

that this structure is also due to threshold effects because of the emergence of new scattering channels. In addition, resonance phenomena contribute to the oscillatory structure. However, if one again assumes a velocity spread of the incident molecules typical for molecular beam experiments [65], the calculated sticking probability becomes rather smooth (solid line in Fig. 7). This means that the quantum effects in the dissociative adsorption probability are hardly visible.

The predicted quantum oscillations have been searched for experimentally by an effusive beam experiment for an angle of incidence of 15° [15, 66], but no oscillations could be detected. As already pointed out, surface imperfections at a reactive substrate such as adatoms or steps reduce the coherence of the scattering process and thus smooth out the oscillatory structure [10, 67]. But more importantly, also the angle of incidence has a decisive influence on the symmetry and the scattering intensities [14]. The calculations were done for normal incidence while the experiment was done for non-normal incidence [15, 66]. At non-normal incidence, the number of symmetrically equivalent diffraction channels is reduced compared to normal incidence. This makes the effect of the opening up of new diffraction channels less dramatic and thus also smoothes the adsorption probabilities.

Experiment [65] and theory agree well, as far as the qualitative trend of the adsorption probability as a function of the kinetic energy is concerned. First there is an initial decrease, and after a minimum the sticking probability rises again. The initial decrease of the sticking probability is typical for H_2 adsorption at transition metal surfaces [15, 65, 68–70]. In these systems, the PES shows purely attractive paths towards dissociative adsorption, but the majority of reaction paths for different molecular orientations and impact points exhibits energetic barriers hindering the dissociation. However, at low kinetic energies most impinging molecules are steered towards the attractive dissociation channel leading to a high adsorption probability. This *steering effect* [13, 71, 72] is suppressed at higher kinetic energies causing the decrease in the adsorption probability.

While diffraction is a consequence of the periodicity of the surface, there are also more local quantum effects occurring within the surface unit cell, in particular if the wave function has to propagate through a narrow transition state. The consequences of such a situation will be illustrated using simple low-dimensional model calculations [17]. In Fig. 8a, an idealized two-dimensional potential energy surface for activated adsorption is plotted as a function of one lateral coordinate and a reaction path coordinate. The minimum barrier has a height. This PES has features appropriate for, e.g., the hydrogen dissociation at the (2×2) sulfur covered $\text{Pd}(100)$ surface [48, 73]: The minimum barrier has a height of 0.09 eV, the adsorption energy is $E_{ad} = 1$ eV, and the square surface unit cell has a lattice constant of $a = 5.5$ Å.

The calculated dissociation probability at such a surface is plotted Fig. 8b. The classical sticking probability

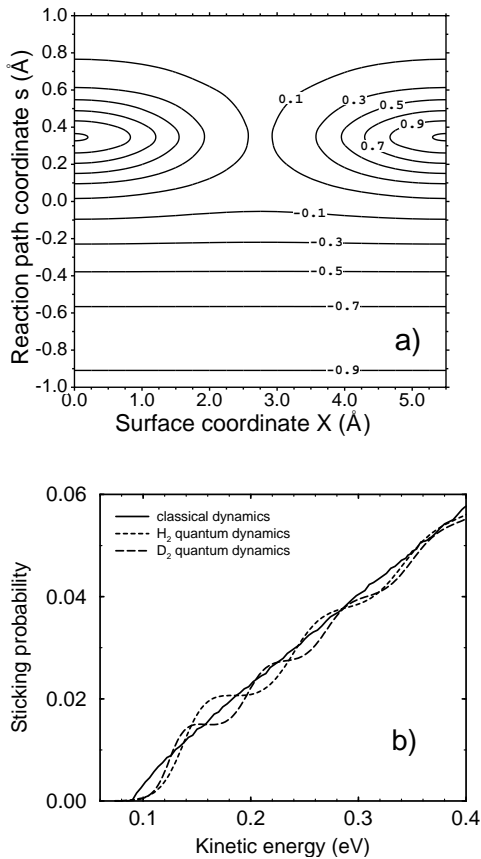


FIG. 8: Activated dissociation of molecular hydrogen at a two-dimensional corrugated surface. a) potential energy surface, b) sticking probability versus kinetic energy for a hydrogen beam under normal incidence. Full line: classical sticking probability which is independent of the mass as a function of the kinetic energy [14]; dashed line: H_2 quantum sticking probability; long-dashed line: D_2 quantum sticking probability [17].

is compared to the quantum sticking probabilities of the hydrogen isotopes H_2 and D_2 . Please note that there is no isotope effects in the dissociation probability as a function of the kinetic energy for hydrogen moving classically on a PES as long as there are no energy transfer processes to, e.g., substrate phonons [14]. This is caused by the fact that at the same kinetic energy H_2 and D_2 follow exactly the same trajectories in space.

The quantum results show a very regular oscillatory structure as a function of the kinetic energy. This is not due to any resonance phenomenon but rather to the existence of quantized states at the transition state [16, 74]. At the minimum barrier position the wave function has to pass through a narrow valley of the corrugated PES. This leads to a localisation of the wave function and thereby to a quantization of the allowed states that can pass through this valley. In the harmonic approximation the energy levels correspond to harmonic oscillator eigenstates which are equidistant in energy. Their spacing $\hbar\omega$ is determined by the curvature of the PES in the

coordinates perpendicular to the reaction path. For H_2 passing through the transition state shown in Fig. 8a, the curvature of the potential perpendicular to the reaction path corresponds to a frequency of $\hbar\omega = 104$ meV. And indeed, the oscillations in the H_2 sticking probability exhibit a period of about 100 meV.

The level spacing of the quantized states depends on the mass of the traversing particles. For D_2 the energetic separation between the quantized states at the transition state is smaller by a factor $1/\sqrt{2}$ compared to H_2 . This is indeed reflected in Fig. 8b by the smaller period of the oscillations in the quantum sticking probability.

The existence of quantized states is closely related to the zero-point energies. Because of the Heisenberg uncertainty principle, there is a minimum energy required for any localized quantum state, namely the zero-point energy. For a harmonic oscillator, this zero-point energy is given by $\hbar\omega/2$. It leads to an effectively higher minimum barrier for the quantum propagation through a transition state region. Consequently, the onset of sticking occurs at higher energies in the quantum calculation than in the classical calculations (see Fig. 8b). However, this onset is not shifted by $\hbar\omega/2$, but by a smaller amount. This is caused by another quantum phenomenon: tunneling. Quantum mechanically particles can also traverse a barrier region for energies below the minimum barrier height. This promoting effect partially counterbalances the hindering effect of the zero-point energies.

Figure 8b demonstrates that the quantum sticking probabilities oscillate around the classical result which means that tunneling and quantization effects almost cancel each other on the average. In addition, if more degrees of freedom are considered, there will be further quantization effects. The combined effect will be a smoothening of the oscillatory structure. Indeed, in six-dimensional quantum calculations of the dissociative adsorption of H_2 on $\text{Cu}(100)$ [43], hardly any steplike structure is visible in the adsorption probability. Therefore it is almost very hard to detect these quantum effects in molecular beam experiments because of limited energetic resolution of the beams and the unavoidable existence of surface imperfections.

VI. CONCLUSIONS

In this review, I have presented an overview over the quantum effects in the interaction dynamics of atoms and molecules at surfaces. They are of particular importance for light atoms and molecules such as helium or hydrogen. The quantum nature of the substrate phonons leads to the phenomenon of elastic scattering at surfaces. This leads to trapping probabilities that are less than one in the non-activated sticking of weakly bound species at surfaces.

Another quantum effect, namely diffraction, is a consequence of the periodicity of surfaces together with elastic scattering. It occurs when the de Broglie wavelength of

the incident beam is of the order of the lattice spacing of the substrate and can be used as a tool to determine surface structures.

The opening up of new scattering channels leads to an oscillatory structure in the intensities of the diffraction peaks and in the dissociative adsorption probabilities of H_2 at reactive surfaces. Furthermore, there are quan-

tum effects due to the existence of quantized states at the transition states of the multidimensional potential energy surface. However, all these additional quantum effects are suppressed by substrate imperfections and surface temperature effects. Hence they can hardly be resolved in experiments.

-
- [1] C. B. Duke and E. W. Plummer, editors, *Frontiers in Surface and Interface Science*, North-Holland, 2002.
- [2] E. Hulpke, editor, *Helium Atom Scattering from Surfaces*, volume 27 of *Springer Series in Surface Sciences*, Springer, Berlin, 1992.
- [3] D. Fariás and K.-H. Rieder, *Rep. Prog. Phys.* **61**, 1575 (1998).
- [4] H. Schlichting, D. Menzel, T. Brunner, W. Brenig, and J. C. Tully, *Phys. Rev. Lett.* **60**, 2515 (1988).
- [5] H. Schlichting, D. Menzel, T. Brunner, and W. Brenig, *J. Chem. Phys.* **97**, 4453 (1992).
- [6] R. Sedlmeir and W. Brenig, *Z. Phys. B* **36**, 245 (1980).
- [7] W. Brenig, *Z. Phys. B* **36**, 227 (1980).
- [8] F. Shimizu, *Phys. Rev. Lett.* **86**, 987 (2001).
- [9] H. Friedrich, G. Jacoby, and C. G. Meiter, *Phys. Rev. B* **65**, 032902 (2002).
- [10] A. Groß and M. Scheffler, *Chem. Phys. Lett.* **263**, 567 (1996).
- [11] D. Cvetko, A. Morgante, A. Santaniello, and F. Tomasini, *J. Chem. Phys.* **104**, 7778 (1996).
- [12] M. F. Bertino, F. Hofmann, and J. P. Toennies, *J. Chem. Phys.* **106**, 4327 (1997).
- [13] A. Groß, S. Wilke, and M. Scheffler, *Phys. Rev. Lett.* **75**, 2718 (1995).
- [14] A. Groß and M. Scheffler, *Phys. Rev. B* **57**, 2493 (1998).
- [15] C. T. Rettner and D. J. Auerbach, *Chem. Phys. Lett.* **253**, 236 (1996).
- [16] A. D. Kinnersley, G. R. Darling, S. Holloway, and B. Hammer, *Surf. Sci.* **364**, 219 (1996).
- [17] A. Groß, *J. Chem. Phys.* **110**, 8696 (1999).
- [18] I. Estermann and O. Stern, *Z. Phys.* **61**, 95 (1930).
- [19] B. Gumhalter, *Phys. Rep.* **351**, 1 (2001).
- [20] R. Frisch and O. Stern, *Z. Phys.* **84**, 430 (1933).
- [21] M. Pating, D. Fariás, and K.-H. Rieder, *Surf. Sci.* **429**, L503 (1999).
- [22] R. G. Rowe and G. Ehrlich, *J. Chem. Phys.*, 4648 (1975).
- [23] G. Brusdeylins and J. P. Toennies, *Surf. Sci.* **126**, 647 (1983).
- [24] J. Lapujoulade, Y. Lecruer, M. Lefort, Y. Lejay, and E. Maurel, *Surf. Sci.* **103**, L85 (1981).
- [25] M. F. Bertino and D. Fariás, *J. Phys.: Condens. Matter* **14**, 6037 (2002).
- [26] K. B. Whaley, C.-F. Yu, C. S. Hogg, J. C. Light, and S. Sibener, *J. Chem. Phys.* **83**, 4235 (1985).
- [27] A. Groß, *Theoretical surface science – A microscopic perspective*, Springer, Berlin, 2002.
- [28] R. W. Fuller, S. M. Harris, and E. L. Slaggie, *Am. J. Phys.* **31**, 431 (1963).
- [29] W. Brenig, *Z. Phys. B* **36**, 81 (1979).
- [30] J. Böheim and W. Brenig, *Z. Phys. B* **41**, 243 (1981).
- [31] I. A. Yu et al., *Phys. Rev. Lett.* **71**, 1589 (1993).
- [32] C. Eltschka, H. Friedrich, and M. J. Moritz, *Phys. Rev. Lett.* **86**, 2693 (2001).
- [33] R. Newton, *Scattering Theory of Waves and Particles*, Springer, New York, second edition, 1982.
- [34] J. A. Fleck, J. R. Morris, and M. D. Feit, *Appl. Phys.* **10**, 129 (1976).
- [35] H. Tal-Ezer and R. Kosloff, *J. Chem. Phys.* **81**, 3967 (1984).
- [36] G.-J. Kroes, *Prog. Surf. Sci.* **60**, 1 (1999).
- [37] A. Groß, *Surf. Sci. Rep.* **32**, 291 (1998).
- [38] A. Groß, *Surf. Sci.* **500**, 347 (2002).
- [39] G. Kresse and J. Furthmüller, *Phys. Rev. B* **54**, 11169 (1996).
- [40] G. Kresse and D. Joubert, *Phys. Rev. B* **59**, 1758 (1999).
- [41] B. Hammer, L. B. Hansen, and J. K. Nørskov, *Phys. Rev. B* **59**, 7413 (1999).
- [42] B. Kohler, S. Wilke, M. Scheffler, R. Kouba, and C. Ambrosch-Draxl, *Comput. Phys. Commun.* **94**, 31 (1996).
- [43] G.-J. Kroes, E. J. Baerends, and R. C. Mowrey, *Phys. Rev. Lett.* **78**, 3583 (1997).
- [44] A. Groß, C.-M. Wei, and M. Scheffler, *Surf. Sci.* **416**, L1095 (1998).
- [45] A. Eichler, J. Hafner, A. Groß, and M. Scheffler, *Phys. Rev. B* **59**, 13297 (1999).
- [46] Y. Miura, H. Kasai, and W. Diño, *J. Phys.: Condens. Matter* **14**, L479 (2002).
- [47] W. Brenig and M. F. Hilf, *J. Phys. Condens. Mat.* **13**, R61 (2001).
- [48] S. Wilke, D. Hennig, R. Löber, M. Methfessel, and M. Scheffler, *Surf. Sci.* **307**, 76 (1994).
- [49] S. Wilke and M. Scheffler, *Phys. Rev. B* **53**, 4926 (1996).
- [50] W. Dong and J. Hafner, *Phys. Rev. B* **56**, 15396 (1997).
- [51] V. Ledentu, W. Dong, and P. Sautet, *Surf. Sci.* **412**, 518 (1998).
- [52] H. F. Busnengo, W. Dong, and A. Salin, *Chem. Phys. Lett.* **320**, 328 (2000).
- [53] C. Crespos, H. F. Busnengo, W. Dong, and A. Salin, *J. Chem. Phys.* **114**, 10954 (2001).
- [54] H. F. Busnengo et al., *Chem. Phys. Lett.* **356**, 515 (2002).
- [55] H. F. Di Cesare, M. A. Busnengo, W. Dong, and A. Salin, *J. Chem. Phys.* **118**, 11226 (2003).
- [56] S. Wilke and M. Scheffler, *Surf. Sci.* **329**, L605 (1995).
- [57] K. Christmann, *Surf. Sci. Rep.* **9**, 1 (1988).
- [58] G. R. Darling and S. Holloway, *Rep. Prog. Phys.* **58**, 1595 (1995).
- [59] W. Brenig, T. Brunner, A. Groß, and R. Russ, *Z. Phys. B* **93**, 91 (1993).
- [60] W. Brenig and R. Russ, *Surf. Sci.* **315**, 195 (1994).
- [61] U. Garibaldi, A. C. Levi, R. Spadacini, and G. E. Tommei, *Surf. Sci.* **48**, 649 (1995).
- [62] S. Andersson, L. Wilzen, M. Persson, and J. Harris, *Phys. Rev. B* **40**, 8146 (1989).

- [63] A. Groß and M. Scheffler, *J. Vac. Sci. Technol. A* **15**, 1624 (1997).
- [64] E. G. McRae, *Rev. Mod. Phys.* **51**, 541 (1979).
- [65] K. D. Rendulic, G. Anger, and A. Winkler, *Surf. Sci.* **208**, 404 (1989).
- [66] C. T. Rettner and D. J. Auerbach, *Phys. Rev. Lett.* **77**, 404 (1996).
- [67] A. Groß and M. Scheffler, *Phys. Rev. Lett.* **77**, 405 (1996).
- [68] K. D. Rendulic and A. Winkler, *Surf. Sci.* **299/300**, 261 (1994).
- [69] M. Beutl, M. Riedler, and K. D. Rendulic, *Chem. Phys. Lett.* **256**, 33 (1996).
- [70] M. Gostein and G. O. Sitz, *J. Chem. Phys.* **106**, 7378 (1997).
- [71] D. A. King, *CRC Crit. Rev. Solid State Mater. Sci.* **7**, 167 (1978).
- [72] M. Kay, G. R. Darling, S. Holloway, J. A. White, and D. M. Bird, *Chem. Phys. Lett.* **245**, 311 (1995).
- [73] C. M. Wei, A. Groß, and M. Scheffler, *Phys. Rev. B* **57**, 15572 (1998).
- [74] D. C. Chatfield, R. S. Friedman, and D. G. Truhlar, *Faraday Discuss.* **91**, 289 (1991).